Improving RF-Based Device-Free Passive Localization In Cluttered Indoor Environments Through Probabilistic Classification Methods

Chenren Xu
WINLAB, Rutgers University
671 Route 1 South
North Brunswick, NJ 08902
lendlice@winlab.rutgers.edu

Bernhard Firner
WINLAB, Rutgers University
671 Route 1 South
North Brunswick, NJ 08902
bfirner@winlab.rutgers.edu

Yanyong Zhang
WINLAB, Rutgers University
671 Route 1 South
North Brunswick, NJ 08902
yyzhang@winlab.rutgers.edu

Richard Howard
WINLAB, Rutgers University
671 Route 1 South
North Brunswick, NJ 08902
reh@winlab.rutgers.edu

Jun Li
WINLAB, Rutgers University
671 Route 1 South
North Brunswick, NJ 08902
jonjunli@winlab.rutgers.edu

Xiaodong Lin
MSIS, Rutgers University
252 Janice H. Levin Hall
Piscataway, NJ 08854
lin@business.rutgers.edu

ABSTRACT

Radio frequency based device-free passive localization has been proposed as an alternative to indoor localization because it does not require subjects to wear a radio device. This technique observes how people disturb the pattern of radio waves in an indoor space and derives their positions accordingly.

The well-known multipath effect makes this problem very challenging, because in a complex environment it is impractical to have enough knowledge to be able to accurately model the effects of a subject on the surrounding radio links. In addition, even minor changes in the environment over time change radio propagation sufficiently to invalidate the datasets needed by simple fingerprint-based methods. In this paper, we develop a fingerprinting-based method using probabilistic classification approaches based on discriminant analysis. We also devise ways to mitigate the error caused by multipath effect in data collection, further boosting the classification likelihood.

We validate our method in a one-bedroom apartment that has 8 transmitters, 8 receivers, and a total of 32 cells that can be occupied. We show that our method can correctly estimate the occupied cell with a likelihood of 97.2%. Further, we show that the accuracy remains high, even when we significantly reduce the training overhead, consider fewer radio devices, or conduct a test one month later after the training. We also show that our method can be used to track a person in motion and to localize multiple people with high accuracies. Finally, we deploy our method in a completely different commercial environment with two times the area achieving a cell estimation accuracy of 93.8% as an evidence of applicability to multiple environments.

Categories and Subject Descriptors

C.3 [**Special-Purpose and Application-Based Systems**]: Real-time and embedded systems; G.3 [**Probability and Statistics**]: Probabilistic algorithms

General Terms

Algorithm, Experimentation, Measurement

Keywords

Device-free Passive Localization, Discriminant Analysis, Multipath, RSS footprint

1. INTRODUCTION

There is growing interest in incorporating automatic "intelligence" in our homes and offices using a dense array of wireless radio/sensor nodes. Central to this intelligence is often the need to localize and track people in indoor environments. Many radio frequency (RF) based localization techniques have been proposed, such as those discussed in [1, 18, 5, 7, 12, 14, 19, 8, 10, 4, 20, 9, 15]. Most of these techniques, however, require the subjects to carry wireless devices, and are referred to as device-based active localization. This requirement has several inherent disadvantages. First, tracking stops whenever the device is detached from the subject either accidentally or intentionally. Second, for applications such as elder care, we cannot assume the subjects will always agree or remember to carry the device.

Recognizing these limitations, the community has started the discussion on RF-based device-free passive (DfP) localization techniques [21]. Compared to its active localization counterpart, DfP offers a lower cost solution as it does not require the participation of the subject and uses low-power RF devices that may already be available in our home/office environment. In DfP localization, we capture the change of the RF signals caused by the subject and try to derive his/her location based upon this change.

Deriving a subject's location from the RSS change caused by the subject, however, is a challenging task, mainly due to the well-known "multi-path" effect [11] that is caused by the reflection and diffraction of the RF signal from subjects and objects in the environment.

(a)

(b)

(c)
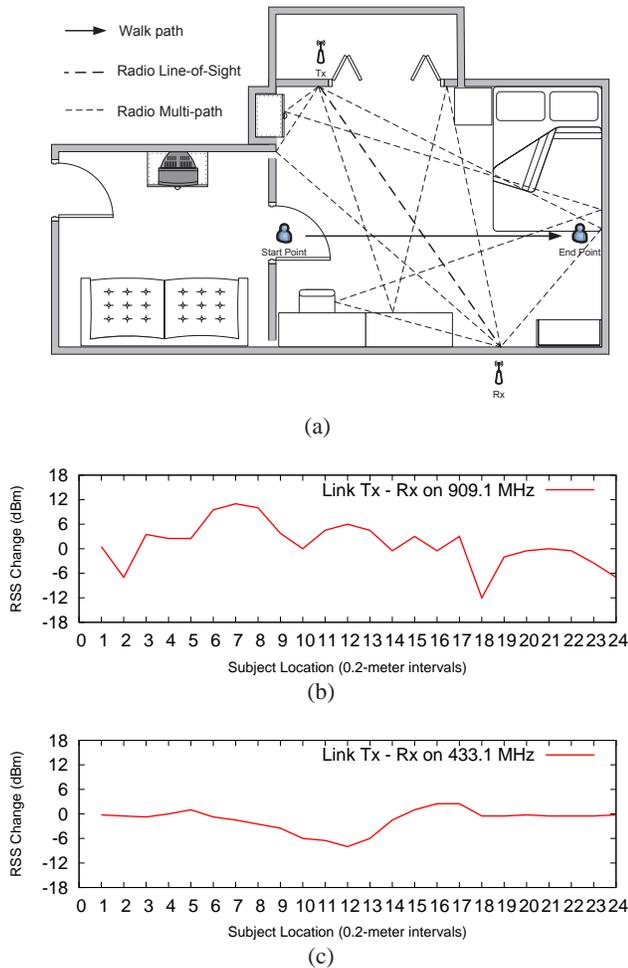
Figure 1: (a) shows the indoor environment in which the radio link has one LoS and four NLoS components; (b) and (c) show the fluctuation of RSS changes between Tx and Rx when the radios operate at 909.1 MHz and 433.1 MHz respectively.

Let us look at a simple experiment to understand the effect of the multipath problem. Figure 1(a) shows the topology of a one-bedroom apartment in which we conduct our experiments. We have one transmitter (Tx in the picture) and one receiver (Rx in the picture), and this radio link has one Line-of-Sight (LoS) component and four Non-Line-of-Sight (NLoS) (or, multipath) components. We only show four NLoS components for simplicity; in reality there are many more present. A person walks from the marked "Start Point" to the marked "End Point". During the movement, we record the received signal strength (RSS) at the receiver (operating at 909.1 MHz), and report the differences between these values and the RSS values when the subject is absent in Figure 1(b). Figure 1(b) shows that the person's effect on the RSS value is random and unpredictable – we observe RSS decreases at different levels, and sometimes we even observe an RSS increase. Figure 1(b) also shows that changes from motion relative to the LoS and NLoS components can be far larger when the subject is not on the LoS than when he is – the variation is as high as 10 db from location 17 to location 18 over a distance of less than 20 cm where the person is

not crossing the LoS of the link. Finally, we note that the multipath effect is affected by many factors. Figure 1(c) shows a completely different behavior when the radio frequency is set to 433.1 MHz.

Many earlier DfP localization techniques either ignored multipath, or failed to treat multipath carefully enough. For example, radio tomography proposed in [16] tries to calculate a subject's location based upon the signal attenuation when the subject is blocking the LoS of the link. These schemes assume there is a direct relationship between a subject's location and the impact on radio signals. They will have good localization results either outdoor or in an empty room with little multipath. In a cluttered room, which is more common in real life than empty rooms, this assumption does not hold. In [21, 13], the authors acknowledge the importance of multipath, and propose a fingerprinting-based approach in which they first collect a radio map with the subject present in a few pre-determined locations, and then map the test location to one of these trained locations based upon observed radio signals. While the fingerprinting approach is certainly a better fit for indoor DfP localization, the localization algorithm in [21, 13] adopts a point-based simplistic minimum Euclidean distance based matching algorithm, which is only practical when the training locations are sparse and the test location closely matches one of the training locations. As training points become denser, classification difficulty will grow significantly.

In this paper, we take on the challenge and strive to improve the performance of DfP localization. Considering the complexity of multipath, *we choose to adopt the fingerprinting approach, and try to achieve good results when we have dense training locations, and random test locations.* We believe these requirements are crucial to many smart home applications such as infant care or elder care. We achieve improved results with the following two optimizations. First, we apply discriminant analysis to the classification problem based on the assumption that the covariates follow a multivariate Gaussian distribution. We validate the assumption of Gaussian distribution through experimental data as well as theoretical approximations. Second, in collecting radio signal readings, we adopt various ways to mitigate the multipath effect so that signal variations within a short distance become smoother. This can increase the distance between classes and further lead to higher classification likelihood. Specifically, our study has the following contributions:

- We derive a sophisticated classification model to better describe the DfP localization problem.

- We improve the quality of data sets by mitigating the error caused by the multipath effect.

- We show that in a one-bedroom apartment of $5 \times 8\ m$ that consists of 32 cells (each being $0.75 \times 0.75\ m$ in size), with 8 transmitters and 8 receivers, we can estimate the occupied cell ID with an accuracy of 97.2%.

- We show that our approach can achieve cell estimation accuracies over 90% in degraded conditions, such as reducing the training overhead (taking 16 data samples per cell instead of 100 samples), reducing the computation overhead, using fewer radio devices (10 devices instead of 16), and conducting tests a month later after the training.

- We show that our approach can be used to track multiple people when they are standing still, walking, sitting, or even lying down. We can also localize multiple people that co-exist in the apartment.
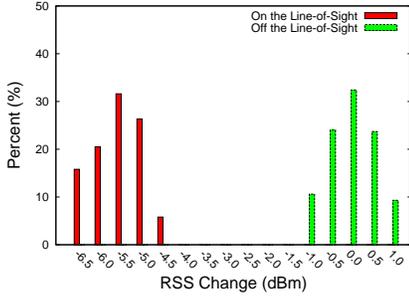
Figure 2: In an outdoor environment, when the radio devices are placed lower than the subject height, the subject causes distinctly different RSS changes for on-LoS cells and off-LoS cells.
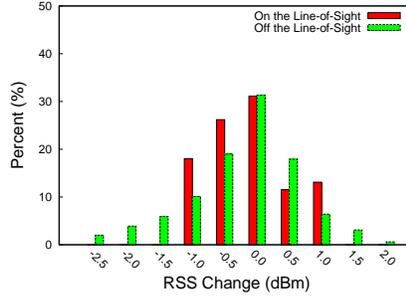
Figure 3: In an outdoor environment, when the radio devices are placed higher than the subject height, the subject causes little effect on the radio signals regardless of his location.
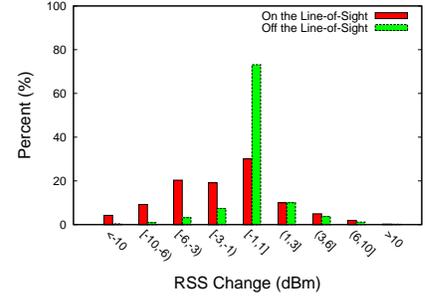
Figure 4: In an indoor environment, when the radio devices are placed below the subject height, the subject's effect on the radio signal is unpredictable with respect to his location.

- We also implement our approach in a much larger commercial office space, and report a cell estimation accuracy of 93.8% from 32 cubicle-size cells.

The rest of the paper is organized as follows. In Section 2, we highlight the challenges faced in indoor DfP localization. We model the system and present our localization algorithm in Section 3. In Section 4, we introduce our experimental setup and methodology. In Section 5, we implement our algorithm in a one-bedroom apartment and report detailed experimental results. We discuss the related studies in Section 6, and conclude the paper in Section 7.

2. CHALLENGES IN A CLUTTERED INDOOR ENVIRONMENT

In this section, through experimentation, we demonstrate the differences between RF-based outdoor and indoor localization, and highlight the challenges posed by indoor environments.

2.1 Outdoor Free Space Localization

We begin our experiments in an open outdoor environment. By setting up a transmitter and a receiver attached on tripods 4.5 meters away from each other in an empty parking lot, we only have a relatively small reflection from the ground. We partition the area into 0.75×0.75 m cells and categorize the cells into two groups: those on the LoS, and those off the LoS. We first record the median of the RSS measurements when the subject is 9 meters away from either device, RSS_E, which represent the base RSS when the subject is absent. Then, we collect 10 continuous RSS readings from each cell while the subject remains stationary in that cell. For each cell, we calculate the RSS change caused by the subject.

We first place the radios such that their height from ground is less than a person's height. In this way, a person can block radio signals more pronouncedly. Figure 2 shows that in this setting, RSS changes in different cells caused by the person clearly fall into two disjoint sets. RSS changes in on-LoS cells are much larger than RSS changes in off-LoS cells. This observation suggests that we may perfectly determine whether the subject is on the LoS or not simply by setting an appropriate threshold for observed RSS changes, which agrees with the observations in earlier studies [16, 3].

Next, we repeat the same experiment, but place the radios above the height of the subject (radios were placed 2 meters above the ground, and the subject is 1.8 meters in height). In this case, the

position of the subject has little effect on the RSS values, as shown in Figure 3. As a result, in the rest of the study, we place the radio devices vertically lower than the subject except when explicitly noted.

2.2 The Multipath Effect

Compared with straightforward localization in the outdoor space, localization in the indoor space is much harder because of the multipath problem. This is particularly true for environments of interest for most applications. Next we will support this statement using experimental observations.

In our indoor experiments, we attach the transmitters and receivers on the wall, 1.2 meters above the floor, which is below most adults and above most of the furniture so that the impact of a subject's presence on the radio signal is maximized. As explained earlier, in an indoor environment, the subject may have an unpredictable impact on the RSS. Figure 4 shows the histogram of RSS changes in different cells. We observe that, when a subject randomly blocks a LoS, *there is only a 50% probability of the signal being attenuated by 1 dB or more*. In other words, 50% of the time the signal will not attenuate or even increase. This observation clearly shows that *the assumption of "blocking LoS" means "attenuation" is misleading in cluttered environments*. On the other hand, the results show that if a subject does not block any LoS, there is a 15% probability that the RSS of a radio link will change more than 3 dB. This further shows the unpredictable nature of the multipath effect.

3. DEVICE-FREE PASSIVE LOCALIZATION THROUGH PROBABILISTIC CLASSIFICATION METHODS (PC-DFP)

As discussed earlier, indoor radio propagation is a very complex phenomenon such that the relationship between a subject's location and the resulting RSS of any radio links in the environment is hard to predict. Thus, statistical rather than deterministic methods are required to extract location information from the measured RF signals. In this section, we discuss in detail our probabilistic classification based device-free passive localization method, *PC-DfP* in short.

3.1 Overview of PC-DfP

We visualize a room as a grid of small square cells with unique addresses or ID numbers. By localizing a subject, we mean to estimate accurately the ID of the cell in which the subject is located.

In our method, we assume there are L radio links in the environment, and there are K cells in a room. In the training phase, we first measure the RSS values for all L radio links when the room is empty (referred to as environmental RSS). Then for each cell k, we collect a set of RSS values with the subject present in this cell. The change between the environmental RSS and the RSS when the subject is in cell k, $[x_{k,1}, ..., x_{k,L}]$, gives the RSS change vector, $\mathbf{x_k}$, for cell k. $\mathbf{x_k}$ is referred to as the *footprint* for cell k. By the end of the training phase, we have obtained RSS footprints for every cell in the room. We build a K-class classifier based on the RSS footprints. Subsequently, in the testing phase, this classifier is used to classify the testing subject with an unknown label (i.e., cell ID).

3.2 Discriminant Analysis

In formulating our classification problem, we label a class k as the state with the subject in the k-th cell, with the associated RSS footprint $\mathbf{x_k}$. For each cell k, we collect the RSS footprint matrix X_k of dimension $\mathbb{R}^{n_k \times L}$, where n_k denotes the number of RSS footprints sampled in the training phase for the k-th cell. The class label is denoted as y_k. The goal of our analysis is to classify the subject with an unknown label into the correct cell ID based on the measured RSS vector.

A large number of classification techniques have been proposed in the literature, including density based approaches. Under the $0 - 1$ loss, the objective is to find the maximizer of the class posterior distribution $P(Y|X)$, where Y is the class label y_k and X is the RSS change vector $\mathbf{x_k}$. A simple application of the Bayes rule gives

$$P(Y = k | X = x) = \frac{f_k(x)\pi_k}{\sum_{j=1}^{K} f_j(x)\pi_j},$$

where $f_k(x)$ is the class-conditional density of X in class $Y = k$, and π_k is the prior probability of class k that sums to 1. Assuming f to be a multivariate Gaussian distribution, we have the classical discriminant analysis. In the remaining of this section, we present a few variations of this technique and describe the rationale for applying them to solve our localization problem.

3.2.1 Minimum Euclidean Distance (MED)

Suppose we have the mean vector $\mu_k \in \mathbb{R}^L$ of the RSS for each class k from the training data. We also have the testing RSS vector x and $\hat{y}$ associated with the unknown cell label to be estimated. The Euclidean distance between x and μ_k is defined as

$$d(x, \mu_k) = \sqrt{\sum_{i=1}^{l} (x_i - \mu_{k_i})^2},$$

where

$$\mu_k = \sum_{i \in class\ k} x_i / n_k.$$

Thus, we have the objective classifier function

$$\hat{y} = argmin_k d(x, \mu_k),$$

as studied in [13].

3.2.2 Linear Discriminant Analysis (LDA)

Linear discriminant analysis aims to find a linear combination of features which characterize or separate two or more classes of subjects [6]. We assume the density of each class k is multivariate Gaussian with mean μ_k and a common covariance matrix Σ:

$$f_k(x) = \frac{1}{(2\pi)^{\frac{L}{2}} |\Sigma|^{\frac{1}{2}}} exp\left[-\frac{1}{2}(x - \mu_k)^T \Sigma^{-1}(x - \mu_k)\right].$$

Applying Bayes rule, we have the objective function

$$\hat{y} = argmax_k f_k(x)\pi_k.$$

In the log-scale, we can write the discriminant function as

$$\delta_k(x) = x^T \Sigma^{-1} \mu_k - \frac{1}{2}\mu_k^T \Sigma^{-1} \mu_k + \log \pi_k,$$

and we find

$$\hat{y} = argmax_k \delta_k(x).$$

Maximization of the discriminant function results in the following parameter updates:

- $\hat{\pi}_k = n_k/n$;

- $\hat{\mu}_k = \sum_{i \in class\ k} x_i / n_k$;

- $\hat{\Sigma} = \sum_{k=1}^{K} \sum_{i \in class\ k} (x_i - \hat{\mu}_k)(x_i - \hat{\mu}_k)^T / (n - K)$;

In our experiment, the number of samples n_k is the same across the all the cells. Therefore the class probability $\pi_j = 1/K$ for all the classes.

3.2.3 Quadratic Discriminant Analysis (QDA)

In practice, it is rare that multiple classes share a common covariance matrix. Quadratic Discriminant Analysis (QDA) is a generalization of LDA that allows different covariance matrices. Such a generalization results in more flexible quadratic decision boundaries comparing to the linear decision boundaries from LDA. The resulting discriminant function is

$$\delta_k(x) = -\frac{1}{2}\log |\Sigma_k| - \frac{1}{2}(x - \mu_k)^T \Sigma_k^{-1}(x - \mu_k) + \log \pi_k.$$

The flexibility of QDA comes with the cost of estimating the different covariance matrices Σ_k. When the dimensionality of x is high, this amounts to a huge increase on the number of parameters to be estimated. Thus in practice, with limited sample size, the simpler LDA is preferable.

3.2.4 Dimension Reduction

In practice, parameter estimation can be challenging even for LDA when data dimension is high. One way to address this problem is through feature selection or dimension reduction. Herein we adopt the linear projection scheme so that the L dimensional vector x can be projected to a q dimensional space via $z = Wx$, where W is a $q \times L$ matrix and $q < L$. For a fixed q, the optimal W is computed by maximizing

$$J(W) = \frac{W^T S_B W}{W^T S_W W},$$

where the within class scatter matrix is

$$S_W = \sum_k (\mu_k - \bar{\mu})(\mu_k - \bar{\mu})^T,$$

and the between class scatter matrix is

$$S_B = \sum_k \sum_{i \in class\ k} (x_i - \mu_k)(x_i - \mu_k)^T.$$

Here $\bar{\mu}$ is the overall mean of x, and μ_k is the mean of the kth class. This leads to solving an eigenvalue problem whose solution is $W_l = S_B^{-1/2} v_l$, where v_l is the lth eigenvector of $S_B^{1/2} S_W^{-1} S_B^{1/2}$. The resulting z is a compact representation of x in a lower dimensional space by projecting the original data to the *first q principal*
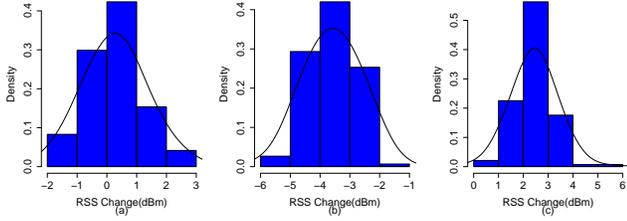
Figure 5: Three histograms for typical experimental RSS change measurements from an arbitrary link when a subject moves randomly within an arbitrary cell. The smooth curve is a log-normal density distribution.

discriminant components. In this way, we can minimize the localization error, reduce the computational cost and prevent the potential over-fitting and singularity problem.

3.3 Gaussian Approximation

In LDA and QDA, we assume that the conditional density given the class label is multivariate Gaussian. In this section, we first present experimental data to support this assumption, and then provide theoretical discussions on why our problem can be approximated by the Gaussian distribution.

Figures 5(a)-(c) show representative histograms for those links with RSS stable (a), attenuated (b) and increased (c). We observe that most of the links fit the log-normal distribution well enough to produce an acceptable fit. As a result, treating RSS values (in power) as Gaussian is a valid assumption. The fact that our results based upon this assumption achieve good classification accuracies (as high as 97% shown in Section 5) is a further support for this assumption.

Next, we explain why we expect that a Gaussian model approximation would work as a first approximation in our classification problem. First, we note that the problem we are addressing is not a typical problem discussed in the literature [11], where the statistics of the multi-path signals at the receiver are considered when either the transmitter or receiver are moved, like in active RF-based localization problems. In passive localization, all the path lengths remain fixed, but the presence of a subject introduces attenuation, scattering, or diffraction of a subset of the multi-path signals. Based upon the geometry of the experimentation room and some simple measurements, we can make analogies, though, to the more typical multipath problem.

In Figure 7(b), it is clear that the major fraction of the links between transmitters and receivers have a substantially clear LoS or at most are obstructed by one relatively transparent interior partition wall. Because of the dominance of the large planar and often perpendicular reflecting surfaces (floor, walls, ceiling), one would expect the multi-path signals to be dominated by LoS and a few, relatively strong components, as seen in [2], along with many components so much smaller than the LoS component that they are insignificant. Finally, we note that in moving around, even a subject that is completely out of the LoS can cause a change in RSS of 10-20 db. This is consistent with a situation in which there are only a small number of multipath components of a magnitude large enough that they could add up constructively and cancel the LoS component to within 10% in amplitude, resulting in a 20db change in energy.

Extending a simplified Rician model [11] to our model would result a dominant LoS signal and a limited number of important mul-

(a)

(b)
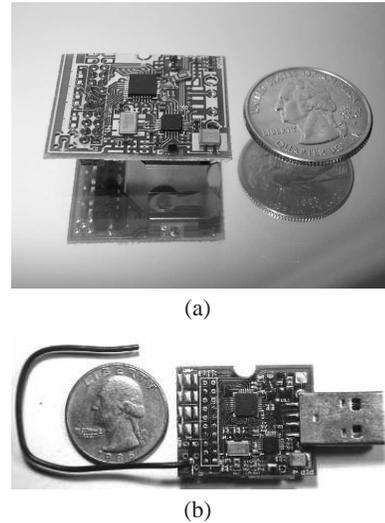
Figure 6: (a) Wireless transmitter. (b) Wireless receiver with USB.

tipath signals whose energy was somewhat smaller in total. This would be the Rician limit where the statistics of the signal are approximately Gaussian, as we have seen. Our results show that this approximation is adequate for our environments.

4. EXPERIMENTAL METHODOLOGY

In our experiments we will show that one or more subjects can be successfully localized in a home/office environment using our PC-DfP method. The system was deployed in two environments: a one bedroom apartment with home furniture and a commercial office space with cubicles and offices. Since most of the experiments were conducted in the first setting, we will focus on the first setting (i.e., the one-bedroom apartment) in the rest of the paper unless otherwise noted. The apartment pictures are shown in Figures 7(a). The apartment is below ground level with a floor area of $5 \times 8\ m$ and a height of $3\ m$. The floor is concrete, the walls are wallboard on wooden studs, and the ceiling is acoustic tile.

Our experimental setup consists of a host PC (Intel i7-640LM 2.13GHz, 3GB RAM) serving as the centralized system, and eight transmitters and eight receivers. Receivers are connected to the PC through a (wireless) USB hub. In our system, each transmitter broadcasts a 10-byte packet every 100 milliseconds. The receivers will forward received packets to the host PC for data collection and analysis. In Section 5, we show that we can reduce the number of radio devices while maintaining good localization results.

4.1 Hardware Description

The radio devices used in our experiments contain a Chipcon CC1100 radio transceiver and a 16-bit Silicon Laboratories C8051-F321 microprocessor powered by a 20 mm diameter lithium coin cell battery, the CR2032. The receivers have a USB connector for loss-free data collection but are otherwise identical to the transmitters. In our experiments, the radio operates in the unlicensed bands at 433.1 MHz or 909.1 MHz. Transmitters use MSK modulation, a 250kbps data rate, and a programmed output power of 0dBm. Each transmitter periodically broadcasts a 10-byte packet (8 bytes of sync and preamble and 2 bytes of payload consisting of transmitter's id and sequence number) ten times per second. When the re-

ceiver receives a packet, it measures the RSS values and wraps the transmitter id, receiver id, RSS, timestamp (on the receiver side) into a "data packet". This packet is sent to the centralized system over direct USB connection or through network hub for data analysis. The transmitter and receiver are shown in Figure 6.

4.2 Experimental Setup

Transmitters and receivers are deployed alternatively one by one along the periphery of the wall depicted in Figure 7(b). Eight transmitters and eight receivers provide 64 independent radio links in total. We virtually partition the room into 32 cells, each roughly $0.75 \times 0.75\ m$ in size. We choose 0.75 m because it is the typical walking step size for adults.

Data Collection: Our method consist of the following two phases:

- Off-line training phase. In the training phase, we will construct the radio map of the room by making 100 measurements in each cell (10 seconds) to determine the RSS footprint. We consider two training strategies. In the first case (*training case A*), the subject will stand at the center of each cell and spin around so that the resulting training data will focus on the cell center but involve different orientations. In the second case (*training case B*), the subject will walk randomly within the cell. Thus, the resulting training data treat all the voxels within that specific cell uniformly and includes all possible orientations.

- On-line testing phase. In the testing phase, the subject (who is different from the subject in the training phase in height and weight) will appear in a random location with a random orientation. In our experiments, we have 100 test locations in each cell, resulting in a total of 3200 test locations. Among the 100 test locations within each cell, 25 of them are the cell center, 25 of them are 0.13 m from the center, 25 of them are 0.25 m from the center, and the other 25 are 0.38 m from the center. For each test location, we take 10 RSS measurements and compute the median value for all the 64 radio links.

4.3 Deployment Cost

Unlike [16, 23], our localization algorithm does not require prior information about the locations of all the radio nodes. Transmitters and receivers can be deployed at random locations. This property enables that PC-DfP can be applied in an environment with no changes to the existing infrastructure. In our experiments, it takes 10 seconds to collect 100 training measurements. Even considering the extra overhead of moving and turning, 30 seconds are sufficient for each cell. **Usually we spend around 15 minutes training the whole deployed region**. Given 32 cells and 100 RSS training measurements for each cell in a 64 dimensional space, it takes 0.044 seconds to estimate the parameters of the classification algorithm, and takes only 0.007 second to estimate the subject location.

Overall, the runtime cost of our method is rather modest. In the results section, we discuss ways of further reducing this cost while maintaining high localization accuracies.

5. RESULTS

In this section, we first discuss performance metrics, and then present detailed experimental results.

5.1 Performance Metrics

The objective of a localization system is to maximize the likelihood of correctly estimating a subject's location and minimize the
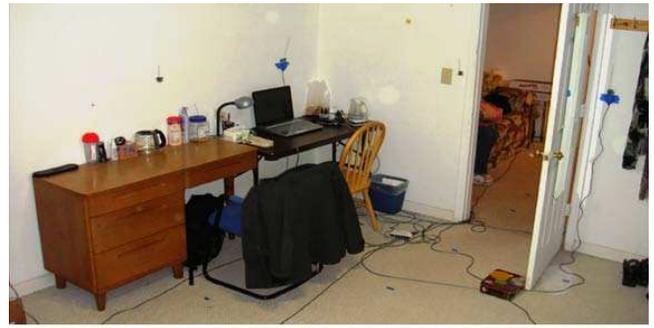
(a)
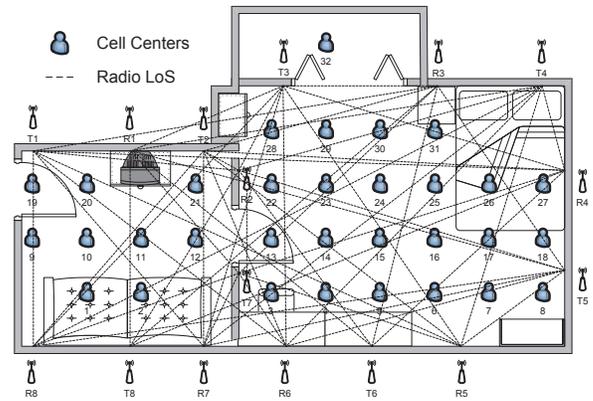
(b)

Figure 7: In (a), we show a rather cluttered one-bedroom deployment region. In (b), we show the experimental topology. The one-bedroom deployment region is partitioned into 32 cells. The center of each cell is marked in the picture. Eight transmitters and eight receivers are deployed. We only show the 64 LoS links here.

average distance between the estimated location and the actual location. For a specific test i, suppose a subject is actually located in cell y_i, and the estimated cell ID is $\hat{y}_i$ by *PC-DfP*. Further suppose we have N_{tst} tests. We thus define the following performance metrics:

- *Cell Estimation Accuracy* is defined as the ratio of successful cell estimations with respect to the total number of estimations, i.e., $\sum_{i=1}^{N_{tst}} I(y_i = \hat{y}_i)/N_{tst}$. In our system, we consider a test successful if the estimated cell is the same as the occupied cell. If the subject is located on the shared boundary

between two adjacent cells, the test is considered successful if the estimated cell is either one of the two bordering cells.

- *Average localization error distance* is defined as the average distance between the actual point location of the subject and the estimated point location (i.e., the center of the estimated cell).

Table 1 summarizes the important parameters used in our experiments. To reiterate, our experiments were conducted in a one-bedroom apartment with the total area of $5 \times 8\ m$, which is divided into 32 cells (size of each cell being $0.75 \times 0.75\ m$). We have 8 transmitters and 8 receivers, resulting in 64 links in total. We note that this number can be made smaller with minimal impact on our localization results. We also note that we anticipate a reasonably large number of sensors/radio devices will be existing in a "smart" home environment. In the training phase, the first author stood in each of these 32 cells, and took 100 RSS measurements. The entire training was finished within 15 minutes by one person.

5.2 Comparing Three Discriminant Analysis Methods

We first compare the results of the three discriminant analysis methods, namely MED, LDA, and QDA. In this set of experiments, the radio frequency is set to 433.1 MHz, and we adopt the training case A. The results are summarized in Table 2.

We observe that LDA performs the best among the three. We expected LDA to outperform MED because it takes into consideration the property of radio propagation. The fact that QDA is the worst of all three, however, is somewhat counter intuitive. After some deliberation, we find out the reason is that QDA requires the estimation of separate covariance matrices for each class, which can lead to over-fitting, especially with a rather limited sample size. The same trend is demonstrated in Figure 8 through the CDF of error distances for the three methods. (We note that QDA does have a slightly shorter tail than LDA.)

In the rest of the performance section, we will thus focus our discussion on LDA.

5.3 Mitigating Multipath Effect

We have mentioned that the multipath effect has an adverse impact on indoor localization, and in this paper, we have devised approaches to mitigate its impact for improved localization results. Specifically, due to multipath, when a subject moves around, we will observe large and abrupt RF variations, even within a cell. Therefore, accurately estimating cell ID based upon the observed RF readings becomes a daunting task. To mitigate this impact, we take the following measures to smooth out the RF variations within a cell.

First, we operate our radios at the unlicensed frequency of 433.1 MHz instead of 909.1 MHz. Intuitively, the wavelength at 433.1 MHz is larger than that at 909.1 MHz, and thus the RF signal has a
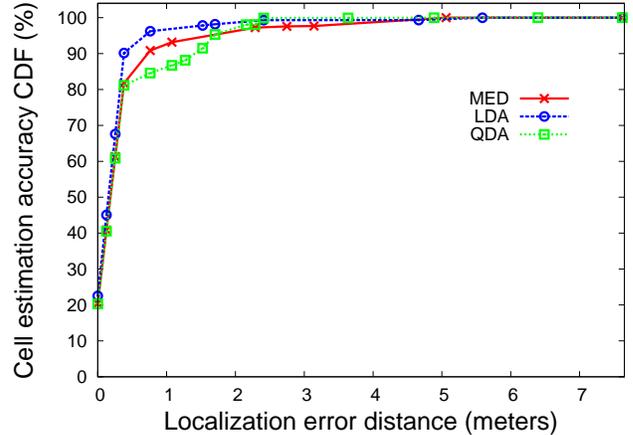
Figure 8: Comparing the CDF of error distances with different discriminant analysis algorithms (MED, LDA, and QDA) at 433.1 MHz.

smoother variation when the subject is moving. We have conducted an experiment to demonstrate this idea. Figure 1(a) shows the experimental setup, and Figures 1(b) and Figures 1(c) shows the RF variation is much smaller at 433.1 MHz than at 909.1 MHz.

Second, in the training phase, instead of standing still at a specific point within a cell and using the measurement at that point to represent the entire cell (as in training case A), we make random movements within that cell, take multiple measurements, and use them collectively for classification, as in training case B in Section 4. In this way, we sample the data for all the voxels with different orientations to average out the multipath effect within each cell.

Table 3 summarizes the LDA results with and without these two optimizations. We also varied the test location in these experiments. In general training case B gives better cell estimation accuracies than training case A. Within each training case, radio frequency of 433.1 MHz gives better results than 909.1 MHz with the node layout shown in Figure 7(b). *In summary, our cell estimation accuracy is as high as 97.2% with the average localization error distance of 0.36 meters.*

5.4 Reducing Training/Testing Overhead

Here we investigate methods for reducing the computing overhead for our algorithm. In this study, we formulate the localization problem as a classification problem that involves a training phase and a testing phase. Suppose we have N training data of L dimensions and K classes, where N is the number of measurements taken in each cell in the training phase, L is the number of radio links in the environment, and K is the number of the cells in the environment. In our default setting, we have $N = 100$, $L = 64$, and $K = 32$.

Parameter	Default value	Meaning
K	32	Number of cells
L	64	Number of radio links
N_{trn}	100	Number of training RSS vector per cell
N_{tst}	100	Number of testing RSS vector per cell

Table 1: System parameters.

Discriminant Analysis Method	Cell Estimation Accuracy (%)	Average Localization Error Distance (m)
MED	81.7	0.55
LDA	90.1	0.44
QDA	81.1	0.53

Table 2: Comparison of the three discriminant analysis methods: MED, LDA, and QDA in training case A.
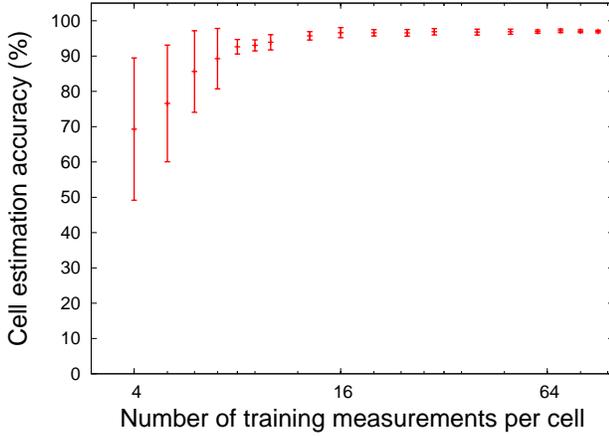
Figure 9: Cell estimation accuracy with 95% confidence interval error bar versus the number of training measurements.
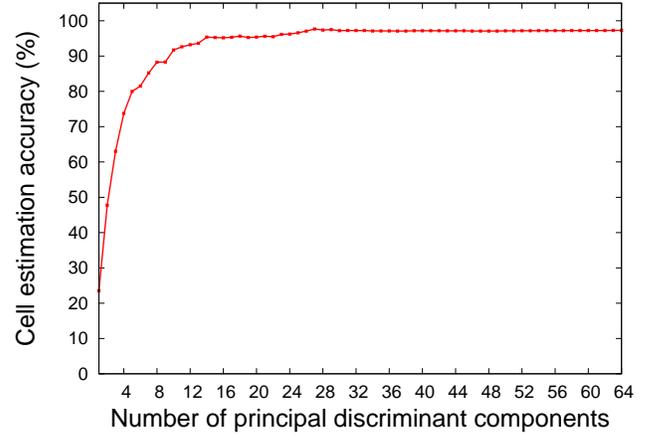
Figure 10: Cell estimation accuracy as a function of the number of most important principal discriminant components.
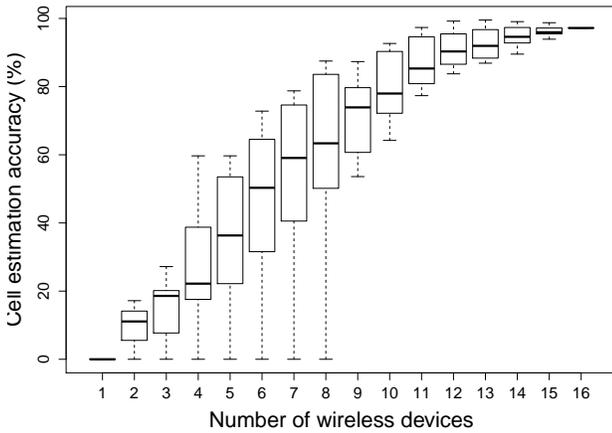
Figure 11: Boxplot of cell estimation accuracy versus the number of wireless devices that are used. For a given number, we show all the possible combinations.

Figure 12: Cell estimation accuracies over one month after the training with different correction approaches.

For LDA, the algorithmic complexity is $O(KNL + K^3)$ in the training phase and $O(KL^2)$ in the testing phase. As K is fixed in our algorithm, we can try to use a smaller N and/or L to reduce the overhead.

First, we look at the possibility of having a smaller N, i.e., fewer training samples. Figure 9 shows the localization results with different training data sizes. We observe that we achieve a cell estimation accuracy of 90% by using 16 training measurements in each cell, and achieve a cell estimation accuracy as high as 90% by only using 8 training measurements in each cell. This will lead to a significant reduction of the training overhead.

Next, we look at the possibility of having a smaller L, i.e., smaller

	433.1 MHz	909.1 MHz
Training case A	90.1%	82.9%
Training case B	97.2%	93.8%

Table 3: LDA cell estimation accuracies improve when the radios work on 433.1 MHz, and adopt the training case B.

data dimensions. To do so, we adopt the optimization technique discussed in Section 3 to select the principal discriminant components for classification purpose. Figure 10 shows that we can achieve the same level of cell estimation accuracy when using only the first 28 principal discriminant components. Such a reduction on data dimension can lead to significant improvement on computation efficiency. If we are willing to relax the requirements for the cell estimation accuracy from 97% down to 90%, then choosing the 10 most principal discriminant components will be sufficient.

5.5 Localizing Subjects with Minimum Number of Radio Nodes

Next, we need to test whether our system can still function if we lose one or more radios. In the experiments, we use a subset of the radio nodes and derive the corresponding localization results, and investigate at what point the cell estimation accuracy will drop below a tolerable level. For example, if we would like to find out the results using 10 radio devices out of the default 16 (8 transmitters and 8 receivers), we would randomly remove 6 devices, and plot the
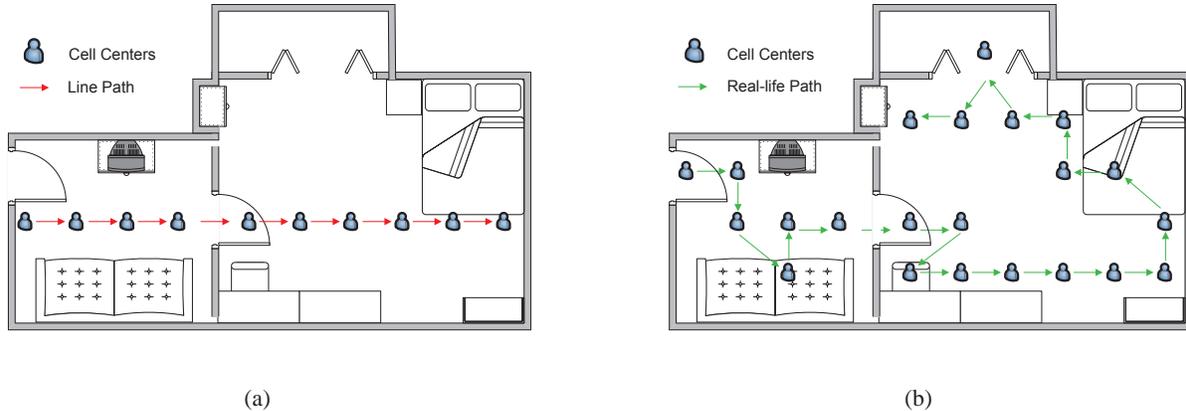
Figure 13: Two mobility paths: (a) a line path, and (b) a real-life path.

localization results for all the possible combinations of transmitters and receivers.

These results are shown in Figure 11. We find that our algorithm can deliver a cell estimation accuracy of 90% when we remove 3 transmitters and 3 receivers in the process. Finally, we note that our system can achieve an even better accuracy (than having all 16 nodes), 99.4%, when three particular devices (i.e., T7, R4 and R6) are removed. Note that we do not reposition the remaining nodes to optimize the results, so this is an overestimate of the number of nodes needed for a given accuracy. Optimizing localization results by systematically removing radio devices (as well as the corresponding links) is a topic for further investigation.

5.6 Using the Same Training Set Over a Long Testing Period

All the results shown above have the testing phase done within three days after training the system. In reality, we are also interested in knowing how well our system will perform if the testing occurs much later in time, which could lead to performance degradation because of changes in the environment or drift in the radio. Different subjects or changes in the same subject could also affect the results.

All the above factors can change the relevance of the original RSS calibration and training. Thus, we need to find an effective correction technique to extend the accuracy of an original calibration over weeks or months. The basic idea is that before each experiment, be it training or testing, we always collect the environmental RSS vector RSS_E when the room is unoccupied. We refer to this vector as RSS_E^{trn} and RSS_E^{tst} for the training and testing phase respectively. This information provides the correction basis for the test data. We can determine when to collect RSS_E^{tst} based upon the subject's life style. For example, it can be collected at noon if he/she works regularly, or at midnight if he/she stays home most of the time.

Using the environmental RSS vector, we propose the following two correction approaches:

- Naive correction: For a simple correction of change over time, we first compute the pairwise difference between the RSS_E^{trn} and RSS_E^{tst}, and record the vector as RSS_E^{bias}. Then we add this bias vector to each RSS vector as the compensation and construct the new test data.

- Truncated correction: We compute RSS_E^{bias} as with naive

correction and set an empirical threshold τ. Then we compare the ith entry $RSS_E^{bias}{}_i$ with τ for $i \in 1, ..., L$. If $| RSS_E^{bias}{}_i | \geq \tau$, then we eliminate that feature (link) from both training data and test data. Otherwise, we compensate the test data for that feature as in naive correction. The rationale behind this approach is that we want to eliminate those links that have experienced a large variation due to environmental instabilities. Since our earlier results (Figure 11) show that our system is robust against missing a few links, we believe removing these links with large fluctuation will not significantly degrade the performance.

We summarize the results in Figure 12. In the case without correction, we do not subtract the environmental RSS from the training/test data. The results show that cell estimation accuracies drop significantly one week after training the system without any correction. With naive correction, we can achieve a cell estimation accuracy of 80% after one month, and truncated correction provides 90% cell estimation accuracy after one month, which is the best among all three.

5.7 Tracking a Moving Subject

Our approach can also be used to track a moving subject. In this set of experiments, the subject moves in the apartment, and we try to estimate which cells he passes during the movement. We choose the longest straight line path and a zigzag path as representatives to test PC-DfP's tracking performance. Specifically, the subject adopted the following two mobility patterns: (1) *line path*, in which the subject walked along a straight line at an average speed of about 3 meters per second (illustrated in Figure 13(a)), and (2) *real-life path*, in which the subject followed a path similar to the path taken in his real life, e.g., he might choose to walk to the bed and lie on the bed for a few seconds, and then walk to the couch and sit down on the couch for a few seconds (illustrated in Figure 13(b)). When the subject moved in the room, we continued to take measurements and estimated which cell he occupied.

We show the localization results in these two cases in Table 4. As expected, when the subject moves along a line path, he can be localized almost as well as when he is stationary, with an cell estimation accuracy of 99.1% and a localization accuracy of 0.3 m. The results for the real-life path are slightly worse (cell estimation accuracy being 91.1%) because there are more complicated movements including walking, lying down, getting up, and sitting. As a

result, more uncertainties are introduced. In particular, the cell estimation accuracy is 86.1% when subject is moving and 98.6% when the subject stays still on bed, chair or sofa. We, however, would like to point out that the average localization error distance in this case, 0.37 m, is still rather good. We note that different paths will lead to varying accuracies as different cells have exhibited different classification accuracies.

In this study, we directly apply our approach to the mobile case without any modification. In our next step, we would like to investigate more sophisticated methods such as taking into consideration the trajectory information.

5.8 Localizing Multiple Subjects When Subject Count Is Known

Next, we extend our method to localizing multiple subjects that coexist in a room if we know the number of subjects. Here, we do not need to do any additional training, and the original training data is sufficient.

In our method, we plug the measured data into the classifier, and retrieve the class label which gives the maximum value from the discriminant functions to estimate the cell number. Similarly, to localize n subjects, we just simply pick n class labels which have the first n maximum values. For multiple subjects localization, we define the cell estimation accuracy as the ratio of the number of the occupied cells that are correctly estimated to the number of subjects. For instance, if there are three subjects and only two of their three cells are correctly estimated, then the cell estimation accuracy will be 66.7%.

We perform 32 independent tests, and show our results in table 5. As expected, the cell estimation accuracy decreases when the number of people increases because more people will cause a higher degree of uncertain interference with radio signals.

5.9 Deploying Our Method to a Larger Office Environment

We have shown that our localization method works well in a home environment where radio devices are installed on the walls. Next, we apply our method to a larger office environment to show that it can easily scale to a different setting. In our experiments, we deploy 13 transmitters and 9 receivers in the first author's office, which is 10×15 m in size. In such an environment, localizing subjects at a 0.75×0.75 m cell granularity is not needed; instead, a cubicle-size cell should be sufficient. Thus, we can still partition the deployed area into 32 cells, as shown in figures 14(a) and 14(b). This deployment has two main differences compared to our original deployment: heterogeneous cell sizes and random radio positions (i.e., not always on the walls). Using the same method, our cell estimation accuracy is 93.8% and the average localization error distance is 1.4 m. This degradation compared to the performance in the one-bedroom apartment can be explained as follows. Intuitively, a larger cell involves more voxels, which result in a large variance for each class. Therefore, for all the classes, there is a higher probability that each pair-wise class will have a larger intersection area, which leads to more classification error.

(a)

(b)

Figure 14: In (a), we show the first author's lab in which we deployed our system. In (b), we show the experimental topology. The office deployment region is partitioned into 32 cubicle-sized cells. Thirteen transmitters and nine receivers are deployed. We show the cell boundaries in this plot.

6. RELATED WORK

In this section, we discuss the related work in device-free passive localization (for stationary subjects) and tracking (for mobile subjects).

Device-free Passive (DfP) Localization: Several DfP approaches have been proposed in the literature. In [21, 13], DfP localization

Different Mobility Path	Cell Estimation Accuracy (%)	Average Localization Error Distance (m)
Line	99.1	0.3
Real-life	91.1	0.37

Table 4: Localization results with two different mobility paths.

Number of People	Cell Estimation Accuracy (%)	Average Localization Error Distance (m)
1	97.2	0.36
2	89.5	0.82
3	83.5	0.89

Table 5: Localization results with respect to number of people in the room when the number is known.

is done through fingerprint matching. A passive radio map is constructed during the training phase by recording RSS measurements with a subject standing at pre-determined locations. During the testing phase, the subject appears in one of these locations, and the system can match the observed RSS readings to the RSS readings from one of the trained locations based upon minimum Euclidean distance. Our method shares the same philosophy with [21, 13] in that multipath is so complex that we cannot understand the direct relationship between a subject's location and the radio signal changes. Instead, we have to train the system first. However, minimum Euclidean distance is shown not to be as efficient as LDA in classification in our study. Further, we have taken special care in the training phase to minimize the RF signal variation within short distances to mitigate the multipath effect. These measures are based upon our in-depth understanding of the radio propagation properties and can lead to much improved localization results.

Radio tomography imaging [16] is a technique to reconstruct the tomographic image for localizing device-free subjects. Here, the authors assume that the relationship between a subject' location and the radio signal variation can be mathematically modeled. In [16, 3], based upon the shadowing effect (RSS is attenuated when the LoS is blocked) caused by the subject, a linear attenuation model and a Sequential Monte Carlo model are proposed respectively. This technique is unlikely to fare well in a cluttered indoor environment because we observed that a person blocking the LoS can only attenuate the RSS with a 50% probability (Section 2).

Device-free Passive Tracking: Several techniques have been proposed to track a moving subject in a passive fashion. In [23, 24], a grid sensor array is deployed on the ceiling for the tracking purpose. An "influential" link is one whose RSS change exceeds a empirical threshold. The authors calculate a subject's location based upon the observation that these influential links tend to cluster around the subject. This work is extended in [22] with triangle sensor array deployment and training information. In VRTI [17], the authors leverage the RSS dynamics caused by the moving subject to generate a radio tomographic imaging for tracking.

Finally, we would like to point out not only fingerprint-based schemes (including ours) need a training phase, but other schemes such as radio tomography and grid sensor array also need a training phase to determine a suitable threshold value to detect if a subject is on the radio LoS.

7. CONCLUSION

In this paper, we present the design, implementation, and evaluation of a device-free passive localization method based on probabilistic classification. We compare three discriminant analysis techniques and find that linear discriminant analysis (LDA) yields much better localization results than minimum Euclidean distance (MED) and quadratic discriminant analysis (QDA). We also propose ways of mitigating the error caused by multipath effect for better localization results, and approaches for correcting training data to facilitate tests much later than the original training. We evaluate our method in a real home environment, rich in multipath. We show that our system can successfully localize a subject with 97% cell estimation accuracy within 0.36 m error distance. Through detailed experiments, we demonstrate that our method can achieve a basic accuracy of over 97%. More importantly, it can maintain an accuracy of over 90% with a substantial reduction in number of radio devices (from 16 down to 10), with far fewer training samples (from 100 to only 16 per cell), or the use of a training set taken a month before testing. In addition, the basic system, without modification, can also be used to track a moving subject or localize multiple sub-

jects. Though originally tested in a small apartment, it performs well in a larger commercial office space.

8. ACKNOWLEDGMENTS

9. REFERENCES

[1] P. Bahl and V. Padmanabhan. Radar: an in-building rf-based user location and tracking system. In *IEEE INFOCOM*, 2000.

[2] D. Cassioli, M. Win, and A. Molisch. A statistical model for the uwb indoor channel. In *IEEE VTC*, 2001.

[3] X. Chen, A. Edelstein, Y. Li, M. Coates, M. Rabbat, and A. Men. Sequential monte carlo for simultaneous passive device-free tracking and sensor localization using received signal strength measurements. In *ACM/IEEE IPSN*, 2011.

[4] K. Chintalapudi, A. Padmanabha Iyer, and V. N. Padmanabhan. Indoor localization without the pain. In *ACM MobiCom*, 2010.

[5] E. Elnahrawy, X. Li, and R. P. Martin. Using area-based presentations and metrics for localization systems in wireless lans. In *IEEE ICN*, 2004.

[6] T. Hastie, R. Tibshirani, and J. H. Friedman. *The Elements of Statistical Learning*. Springer, 2nd edition, 2003.

[7] P. Krishnan, A. Krishnakumar, W.-H. Ju, C. Mallows, and S. Gamt. A system for lease: location estimation assisted by stationary emitters for indoor rf wireless networks. In *IEEE INFOCOM*, 2004.

[8] D. Madigan, E. Einahrawy, R. Martin, W.-H. Ju, P. Krishnan, and A. S. Krishnakumar. Bayesian indoor positioning systems. In *IEEE INFOCOM*, 2005.

[9] L. Ni, Y. Liu, Y. C. Lau, and A. Patil. Landmarc: indoor location sensing using active rfid. In *IEEE PerCom*, 2003.

[10] N. B. Priyantha, A. Chakraborty, and H. Balakrishnan. The cricket location-support system. In *ACM MobiCom*, 2000.

[11] T. Rappaport. *Wireless Communications: Principles and Practice*. Prentice Hall PTR New Jersey, 2nd edition, 2001.

[12] T. Roos, P. Myllymaki, and H. Tirri. A statistical modeling approach to location estimation. *IEEE Transactions on Mobile Computing*, 1(1), 2002.

[13] M. Seifeldin and M. Youssef. A deterministic large-scale device-free passive localization system for wireless environments. In *ACM PETRA*, 2010.

[14] A. Smailagic and D. Kogan. Location sensing and privacy in a context-aware computing environment. *IEEE Wireless Communications*, 9(5), 2002.

[15] R. Want, A. Hopper, V. Falcão, and J. Gibbons. The active badge location system. *ACM Transactions on Information Systems*, 10(1), 1992.

[16] J. Wilson and N. Patwari. Radio tomographic imaging with wireless networks. *IEEE Transactions on Mobile Computing*, 9(5), 2010.

[17] J. Wilson and N. Patwari. See-through walls: Motion tracking using variance-based radio tomography networks. *IEEE Transactions on Mobile Computing*, 10(5), 2011.

[18] K. Woyach, D. Puccinelli, and M. Haenggi. Sensorless sensing in wireless networks: Implementation and measurements. In *IEEE WiOpt*, 2006.

[19] M. Youssef and A. Agrawala. Small-scale compensation for wlan location determination systems. In *IEEE WCNC*, 2003.

[20] M. Youssef and A. Agrawala. The horus wlan location determination system. In *ACM MobiSys*, 2005.

[21] M. Youssef, M. Mah, and A. Agrawala. Challenges: device-free passive localization for wireless environments. In *ACM MobiCom*, 2007.

[22] D. Zhang, Y. Liu, and L. Ni. Rass: A real-time, accurate and scalable system for tracking transceiver-free objects. In *IEEE PerCom*, 2011.

[23] D. Zhang, J. Ma, Q. Chen, and L. M. Ni. An rf-based system for tracking transceiver-free objects. In *IEEE PerCom*, 2007.

[24] D. Zhang and L. M. Ni. Dynamic clustering for tracking multiple transceiver-free objects. In *IEEE PerCom*, 2009.